MULTICOLOR QUANTUM WELL INFRARED PHOTODETECTORS

Meimei Z. Tidrow
Army Research Laboratory
Adelphi, MD 20783

ABSTRACT: Multicolor infrared (IR) detectors are very important to advanced IR sensor systems. An IR detector with multicolor capability can offer a better target discrimination, tracking, and identification, as well as temperature determination. Multicolor IR sensors are also very useful in industry for gas leakage detection, chemical analysis, and for environmental sensing and control. As the IR technology continues to advance, there is a growing demand of multicolor IR detectors for advanced IR sensor systems. Quantum well infrared photodetector (QWIP) is one of the competing technologies that shows very promising potential in infrared detection and imaging. One major advantage of QWIPs is its multicolor detection capability and voltage tunability. Several approaches of achieving multicolor detection, detailed device structures, and performance of multicolor QWIPs will be presented. The multicolor voltage tunability, simultaneous detection capability, nd the Stark Shift effect for fine tuning of the peak etection wavelength will be discussed.

1. Introduction

Infrared (IR) detection has been extensively investigated ever since the discovery of IR radiation in 1800 and utilized both in commercial world and military. The IR spectrum can be divided into short wavelength IR (SWIR, 1 to 3 μm), mid-wavelength IR (MWIR, 3 to 5 μm), long wavlength IR (LWIR, 8 to 12 μm) and very long wavelength IR (VLWIR, > 12 μm). Traditionally, competitive material systems such as indium antimonide (InSb), platinum silicide (PtSi), mercury cadmium telluride (HgCdTe) and arsenic doped silicon (Si: As) have dominated IR detection. PtSi and InSb focal plane arrays (FPAs) have been used in MWIR and HgCdTe FPAs in LWIR. Only extrinsic IR detectors such as Si:As photoconductors has be used at VLWIR. New competition and an evolving market have placed considerable pressure on conventional IR detectors. Stringent system specifications, cost, manufacturability, plus the increasing interest in multicolor imaging, on-chip signal processing, and optical interconnects, have stimulated considerable efforts in alternative technologies. Among the competing technologies are the quantum well infrared photodetectors (QWIPs) based on lattice matched GaAs/AlGaAs and strained layer InGaAs/AlGaAs material systems.

Quantum IR detectors such as HgCdTe and InSb use electron band to band transitions where incoming photons excite electrons in the valence band to the conduction band. The electrons change mobility and are collected at the contact. The detection cutoff wavelength is decided by the band gap and the detection spectrum width is wide since all photons with energy larger than the band gap can make electron transition. QWIPs use intersubband transition instead of interband transition. Intersubband transition in GaAs/AlGaAs multiple quantum well structures was first observed by West and Eglash in 1985.[1] The intersubband transition occurs only in conduction band or valence band depending on the photoexcited carriers being electrons or holes. Quantum well and superlattice structures using intersubband transitions have been widely used in the applications of the optoelectronic devices such as waveguides, modulators, lasers and infrared detectors. The characteristics of these devices are determined by the optical properties, therefore by the intersubband transitions of the quantum well structures.

In n-type QWIPs, the GaAs/AlGaAs system is the most studied and mature system[2]. It uses the fact that by changing the Al concentration x, the bandgap of $Al_xGa_{1-x}As$ can vary from 1.43eV (x=0) to 2.16eV (x=1) at 300K. Using GaAs as quantum well region and AlGaAs as barrier region, confined quantum well structures can be formed when the well width is small. The thickness of the GaAs layer decides the width of the quantum wells and the Aluminum concentration x value decides the barrier height. Molecule beam epitaxy (MBE) is used to precisely lay the atomic layers down to form the quantum wells. The mature GaAs technology ensures the success and the repetition of the material growth. By designing different well width and barrier height, as well as different well and barrier combinations in QWIPs, detection wavelength can be achieved from 3μm to 30μm or even longer. In LWIR region, large size (256x256 and 640x480) QWIP FPAs by Lockheed Martin have been demonstrated with high uniformity, high yield and low cost. Jet Propulsion Laboratory also demonstrated a hand-held IR camera using a 256x256 QWIP FPA with excellent imagery at

9.4μm peak wavelength and 70K operating temperature.

2. Multicolor QWIPs

Besides its wavelength flexibility, one major advantage of QWIPs is its multicolor detection capability and voltage tunability. These properties make QWIPs more competitive than other cooled IR technology when multicolor property is required. The capability to measure infrared radiation in more than a single waveband is very important for IR detection and IR imaging. Detection of multiple infrared wavebands allow determination of the thermal characteristics and special futures of an object. It is also a very important tool for chemical analysis and medical imaging. So far, the multiple waveband measurements have been achieved using separate FPAs with a dichroic filter, a mechanical filter wheel, or a dithering system with a striped filter. Each of these approaches is expensive in terms of size, complexity, and cooling requirements. The QWIP technology can integrate multiple wavebands into separate stacks of a single FPA. This kind of integrated multicolor FPA eliminates the spatial alignment and temporal registration problems that exist whenever separate arrays are used. It also allows the incorporation of the concept of multi-domain smart sensor technology and new signal processing techniques, such as simultaneous detection, and multiple waveband threshold testing. Other advantages of multicolor QWIP FPAs include simpler optical design, reduced size, weight, and power consumption.

Even though multicolor QWIP FPA is still in the developing stage, different quantum well structures have been demonstrated and showed great potential in multicolor FPA applications. Examples of multicolor QWIPs are multi-stack QWIPs[3-5], asymmetrically graded barrier QWIPs[6,7], asymmetric double[8] and triple coupled QWIPs[9], and three-well QWIPs[10]. Highly doped QWIPs are used to achieve electron occupation in two quantum states[11,12]. An extra energy bandpass filter on top of a graded-barrier QWIP is used to select color and control the cutoff wavelength[13]. Most multicolor QWIP structures mentioned here are wavelength tunable by changing the bias voltage. A third terminal has been added to a two-stack QWIP[5] for simultaneous two color detection in MWIR and LWIR. Simultaneous imagery in separate wavebands offers high accuracy band ratio of objects and background scene clutter, especially when the photon flux from these sources varies temporally.

In this presentation, four detailed QWIP structures[8,9,5,14] of achieving multicolor detection are given and their performance discussed. All devices are grown on semi-insulating (001) GaAs substrate using MBE technique. The devices are fabricated using standard photolithography and wet chemical mesa etching. All devices have a 45° facet polished at the back of the substrate for IR coupling. No substrate thinning was made on any of the devices. The photocurrent spectra were measured using a monochrometer and a calibrated globar source. In the dark current and photocurrent measurements, the substrate contact was grounded while positive or negative bias was applied to the top contact of the devices.

2. An asymmetrically double coupled QWIP

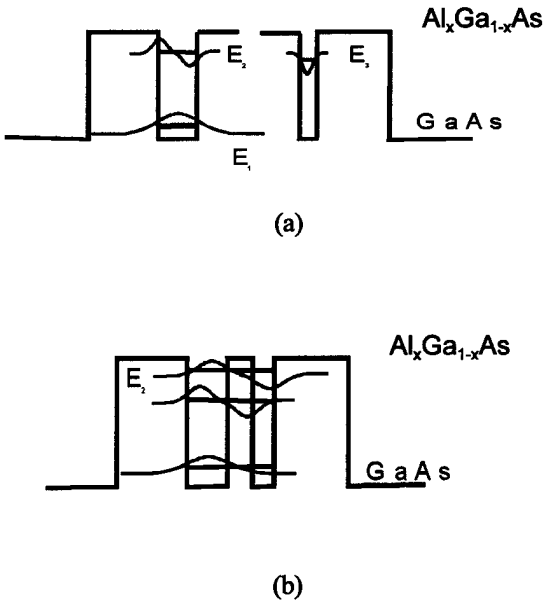

Fig. 1. The energy diagram of the double coupled QWIP (a) before coupling, and (b) after coupling.

The first device is a double coupled quantum well structure contains of 30 periods of double coupled quantum wells of different widths separated by a thin barrier in each period[8]. The well widths for the wide well and the narrow well are 72 Å and 20 Å, respectively. The barriers are made of $Al_{0.31}Ga_{0.69}As$ and

are 40 Å thick between the two asymmetric wells and 500 Å thick between the units. The device is designed to have two subbands E_1 and E_2 in the wide well and one subband E_3 in the narrow well (see figure 1). Due to the strong coupling effect of the asymmetrical quantum wells, three bound states (E_1, E_2, E_3) are formed inside the quantum wells. The wide well is doped and electrons from the first energy state E_1 can be excited by incoming photons to either E_2 or E_3 energy states. Because the parity symmetry is broken in the coupled asymmetric quantum well structure, both transitions can happen.

The dark current and 300 K background window photocurrent with a 36° field of view (FOV) is given in Fig. 2. It is easy to see that the device is background limited (BLIP) at 60 K for bias voltage up to positive 4 V and negative 10 V.

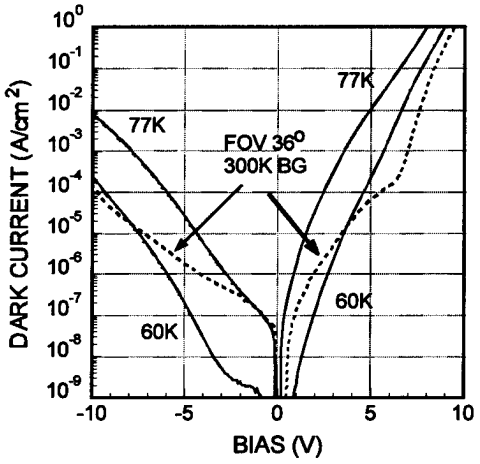

Fig. 2. The dark current of the double coupled QWIP.

Three peak responses have been observed with photocurrent measuremnt. Under positive bias, one peak is observed at 9.6 μm which is in excellent agreement with the FTIR measurement for the intersubband interaction between E_1 and E_2. Since the photon spectrum is proportional to the product of the photon absorption and the hot electron transmission, the transition between E_1 and E_3 is not observed under positive bias due to the small oscillator strength and a small transmission caused by the thick barrier between the coupled quantum well units. At negative bias, both E_1 to E_2 and E_1 to E_3 transitions are observed. According to calculations using a simple linear voltage span assumption, E_3 will align with E_2 at a negative bias of 6.5 V. Above this voltage, E_3 is higher than E_2. Electrons from E_3 can easily tunnel through the 40 Å barrier and form a photocurrent peak around 8.4 μm. A small Stack Shift is observed for the 8.4 μm peak which is associated with the asymmetric coupled quantum wells. With increasing negative bias, the transmission of electrons from E_2 increases and a prominent peak appears at 10.3 μm. This peak wavelength is longer than the original 9.6 μm, which is due to the down shift of the E_2 state as a result of the interaction between E_2 and E_3 when E_3 is higher than E_2. Figure 3 gives an example of the tunability of the detector and their corresponding responsivity. The three detection peaks in fig. 3 are distinctive and well resolved with detection peaks at 8.4 μm, 9.6 μm and 10.3 μm. Multicolor capability and voltage tunability are demonstrated due to the effect of double well coupling. The detection peak is selectable independently among those three wavelengths by tuning the bias voltage.

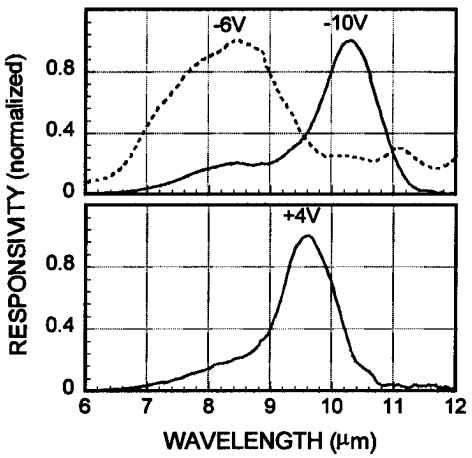

Fig. 3. The normalized responsivity of the three colors under -6V, -10V and +4V.

4. An asymmetrically Triple Coupled QWIP

The second device is a triple coupled QWIP[9]. It is similar to the double coupled QWIP but with three quantum wells formed by an enlarged Si-doped InGaAs quantum well and two undoped GaAs quantum wells separated by two thin AlGaAs barriers. Three bound states (E_1, E_2, E_3) are formed inside the quantum wells

due to the triple coupling of the three quantum wells. The main detection peak wavelength is due to E_1 to E_2 transition, while two secondary detection peaks due to E_1 to E_3 and E_1 to E_C states are also observed, where E_C is the continuum states above the barrier. In addition, a strong quantum confined Stark Shift for the E_1 to E_3 transition is observed in the wavelength range of 8.2 μm to 9.1μm and exhibits a linear dependence of detection peak wavelength shift with the applied bias voltage. This wavelength tunability is highly desirable for IR applications such as target discrimination and temperature determination. The device demonstrated here use triple coupled quantum wells. The large spatial separation of the ground state and the higher energy states effectively enhanced the Stark effect compared with the double coupled QWIP. The dark current density versus bias voltage measured at 40 K, 66 K and 77 K also shows the asymmetrical dark current characteristics under positive and negative bias. Since the effective barrier height under negative bias is smaller than that of the positive bias case, the dark current density is larger under negative bias than the positive bias condition.

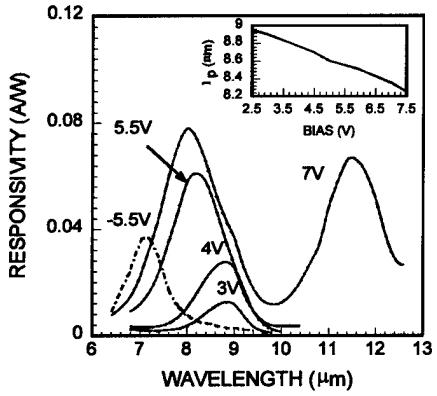

Fig. 4. The voltage tunability of the triple coupled QWIP and the Stark Shift effect shown in the inset.

The responsivity peaks and the bias conditions are given in Fig. 4. The detection peak due to E_1 to E_3 transition is observed starting from 2.5 V bias and increases with bias up to 7 V. The photoresponse due to E_1 to E_2 transition is observed at bias larger than 6 V. The 7.2 μm peak under negative bias is attributed to the bound-to-continuum states transition. A linear bias dependence of the peak detection wavelength due to E_1 to E_3 transition is shown in the inset of Fig. 4, which proves a large quantum confined Stark Shift effect. The tunable wavelength range for E_1 to E_3 transition is found to be 8.2 μm to 9.1μm.

5. A high strain two-stack, two-color QWIP

The third device is a high strain two-stack, two-color QWIP[5]. It consists of two stacks of multiple quantum wells as the active region with a highly doped contact layer in between. The schematic energy band diagram of the device is given in Fig. 5. The first stack is designed to detect the MWIR with 20 periods of 300Å $Al_{0.38}Ga_{0.62}As$ barrier and 24Å $In_{0.35}Ga_{0.65}As$ well sandwiched between two 5Å GaAs layers. The second stack is for the LWIR detection which consists of 20 periods of 500Å $Al_{0.27}Ga_{0.73}As$ barrier and 55Å GaAs well.

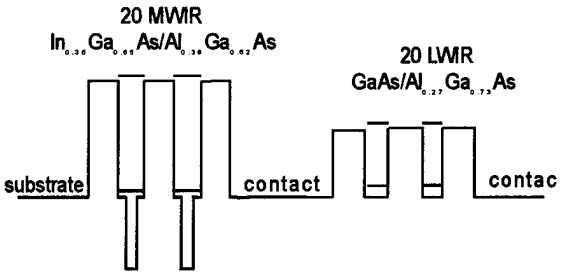

Fig. 5. The energy band diagram of the high strain two-stack two- color QWIP.

The primary concerns of the two-color detection are the difficulty of tuning the detection wavelength to the middle of the MWIR region and the low responsivity of the MWIR stack due to the narrow quantum wells. The device reported here incorporated 35% of indium in the InGaAs well of the MWIR stack which achieved not only peak response at 4.3 μm which is in the middle of the MWIR atmospheric window, but also very low dark current and very high responsivity. Asymmetric (115) X-ray measurements showed very little lattice relaxation with less than 186 parts per million increase of the in-plane lattice constant. The low dark current and the good uniformity of the device also show that the device is of high quality despite the high indium concentration.

Fig. 6 shows the dark current for the MWIR stack measured at 77 K and 122 K, along with the 300 K window current measured at 30 K with a FOV of 180°. The sample is highly uniform and has very low dark current. The BLIP temperature was found to be 125K up to ±2 V and 120 K up to ±3 V. The

dark current at 35 K, 6 6K, and the 300 K window current for the LWIR stack are also measured . The BLIP temperature is around 70 K for bias up to ±2 V with a cutoff wavelength at 10 μm. 77 K operation could be achieved by shifting the cutoff wavelength to 9μm.

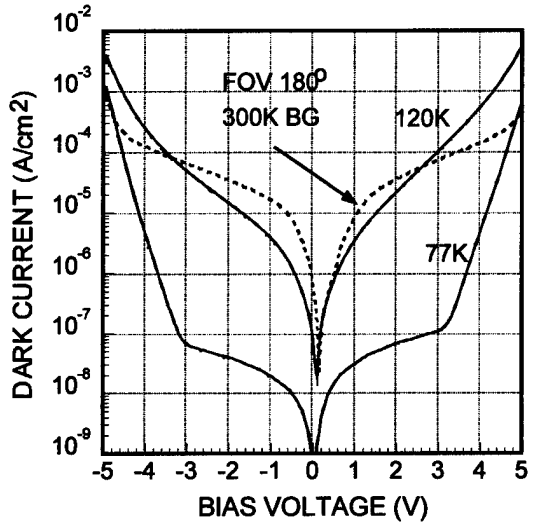

Fig. 6. The dark current of the MWIR stack of the two-stack, two-color QWIP.

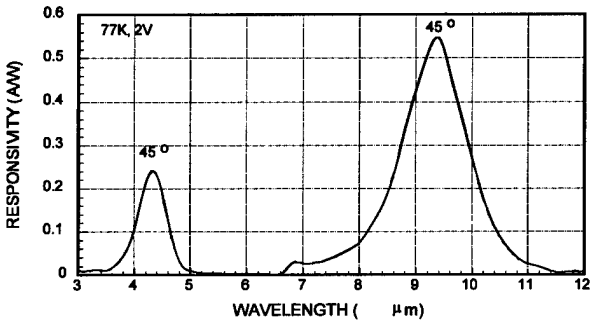

Fig. 7. The spectral responsivity of the two-stack, two-color QWIP with 2 V bias on each stack.

Fig. 7 gives the spectral responsivity for the MWIR and LWIR stacks measured at 77 K with 2 V bias on each stack. The peak wavelengths at 2V are 4.3 μm and 9.4 μm for the MWIR and LWIR, respectively. Fig. 8 shows the peak (4.3 μm) responsivity versus bias for the MWIR stack measured at 77 K. The maximum peak responsivity for the MWIR is 0.65 A/W at 3 V with 45° incidence which gives the highest responsivity with best BLIP temperature reported so far for the MWIR QWIPs. Besides relatively large doping in the well, the enhanced responsivity in the MWIR stack is also high strain related. The compressive strain induced in the 35% InGaAs quantum well leads to a 20% reduction of the electron effective mass compared to no indium case. As a result, the intersubband absorption and hence the photoresponse are expected to increase over the unstrained case with the same well width. Fig. 9 shows the peak responsivity at 9.4 μm versus bias voltage for the LWIR stack measured at 77 K. The responsivity increases linearly with bias up to ±2V and becomes saturated with a maximum value of 0.55 A/W at 2 V with 45° incidence.

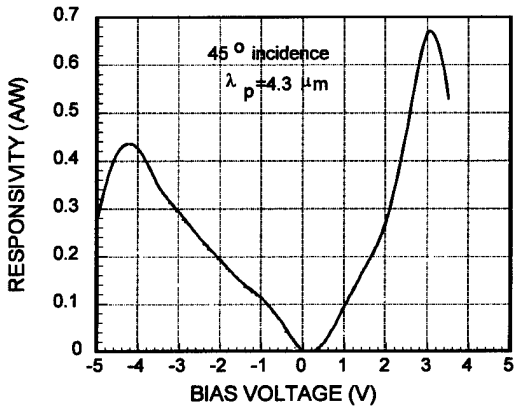

Fig. 8. The peak responsivity of the MWIR stack vs. bias.

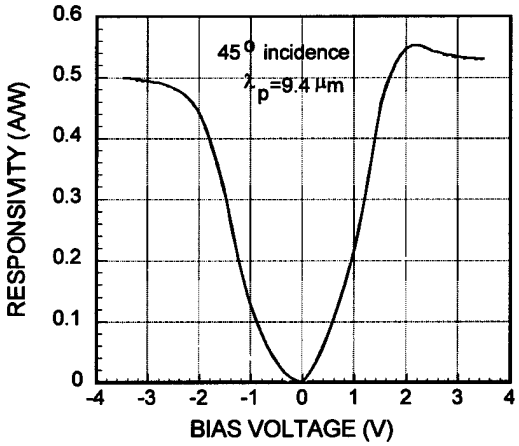

Fig. 9. The peak responsivity of the LWIR stack vs. bias.

6. A four-stack four-color QWIP

The last device described here is a four color detector[14] in which four stacks of quantum well structures with four different detection wavelengths are sandwiched among three contact layers. The peak wavelengths of the four colors are at 4.7 μm, 8.5 μm, 9 μm, and 12.3 μm. The 4.7 μm and 8.5 μm stacks are separated from the 9 μm and 12.3 μm stacks by a middle contact layer and the peak detection wavelengths change within the two two-stack QWIPs are obtained by varying the bias voltage. Four different combinations of two-color simultaneous reading can be achieved. The detector could make simultaneous reading of four colors by adding two extra contact layers to the design with appropriate readout circuitry. By using small number of quantum wells, we are able to use all four stacks for voltage tunable detection with two terminals. The four stacks of QWIPs are designed with variations of the number of QWs, barrier widths, and doping densities. The purpose is to achieve reasonable bias voltage distribution among the stacks without having to bias too high.

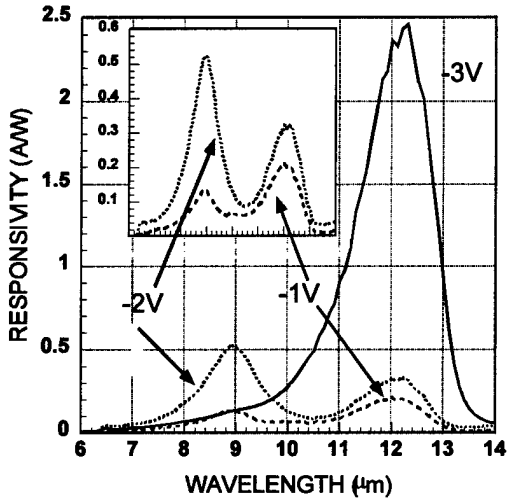

Figure 10. The spectral responsivity of the top two stacks, showing the wavelength tunability by changing the bias.

Figure 10 shows the spectral responsivity of the top two stacks at 40 K under several different biases. There is no middle contact layer between these two stacks, and the two-color detection is achieved by varying the bias voltage. If the two stacks have the same number of QWs, barrier width and doping density, then the impedance of the 9.0 μm stack will be much larger than that of the 12.3 μm stack, and the photoresponse should show up first at small bias. By increasing the number of QWs and the barrier width and reducing the doping in the 12.3 μm stack, the voltage distribution across the two response peaks can be obtained in this stack. For example, both response peaks at 9.0 μm and 12.3 μm were observed at $V_b = -1$ V. When the bias is increased, the dark current of the 12.3 μm stack increases much faster and the voltage drop is mostly on the 9.0 μm stack at –1.5 V. As the bias voltage continues to increase, the 12.3 μm stack finally becomes dominated. This is clearly seen at – 3 V in figure 10, where no obvious 9.0 μm peak appears.

The dark current of this two-stack QWIP was measured at 40 K, 60 K, 70 K and 77 K, along with the 300 K background window current with a field of view (FOV) 180°. The device has background limited infrared photodetection (BLIP) at 70 K up to – 1.65 V and + 1.5 V, at 60 K up to ± 2.5 V. At - 3 V, the photocurrent is dominated by the 12.3 μm stack with a cutoff wavelength at 12.9 μm, as seen from figure 10.

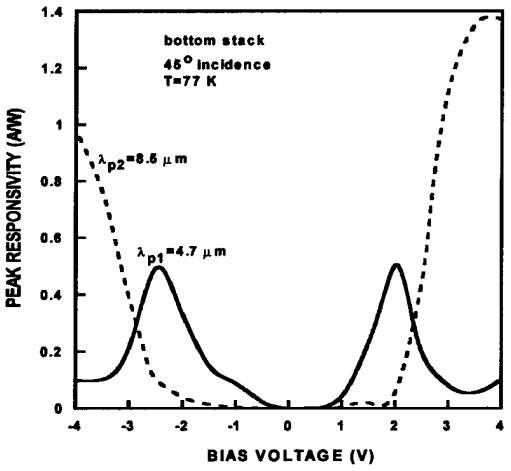

Figure 11. The peak detection of the two color of the bottom two stacks, showing the voltage tunability of this two stacks by changing the bias.

The peak detection wavelengths of the bottom two stacks are at 4.7 μm and 8.5 μm. Figure 11 shows the peak responsivities of bottom stack as a function of bias voltage. At 77 K, the 4.7 μm stack dominates at small bias up to –3 V and + 2.5 V, due

to its high impedance. However, because of the design consideration in which twice as many number of periods as the 4.7 μm stacks (4 periods) are used in the 8.5 μm peak (8 periods), the 8.5 μm stack also shows some photoresponse at low bias. When the bias increases, the responsivity of the 8.5 μm stack increases, and finally becomes dominated. We have measured the dark current of the bottom two stacks at several different temperatures along with the 300K window current with 180° FOV. The BLIP temperature was found to be 110 K up to bias voltages of +1 V and –2 V, 90 K up to +2.5 V and –3.5 V, and 77 K up to -5.6 V and +5 V. Due to the low dark current and high responsivity of this detector, the 4.7 μm shows a stable response at 120 K and 1 V bias with a peak responsivity of 355 mA/W. Clean spectral responsivity is shown even at 150 K and 0.5 V bias with a peak responsivity of 80 mA/W.

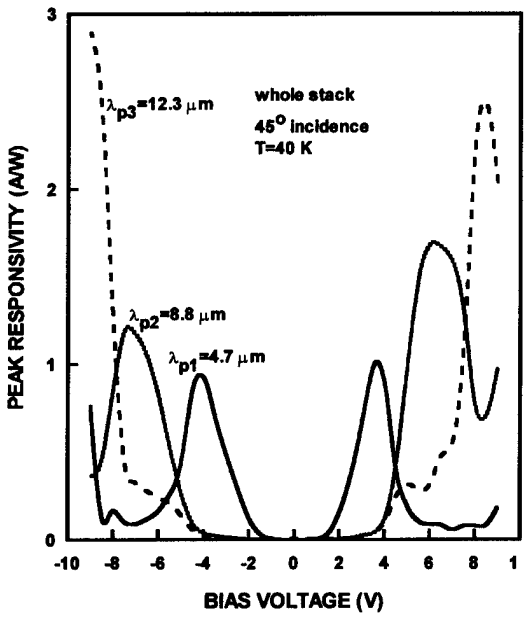

Figure 12. The three peak wavelengths of the whole stack change as a function of bias, showing the tunability of the whole stack.

The voltage tunability of the whole stack as a two-terminal device is shown in figure 12. Because of the existence of the mid-wave stack, the voltage required to turn on the 12.3 μm stack is much higher than that required in the two-stack LW/LW operation. However, special consideration has been given in the detector design to balance the voltage distribution in the four stacks. Therefore, the bias voltage required to turn on the 12.3 μm stack is still much smaller than it would be when each stack uses the same number of periods. The spectral response of the whole stack has three response peaks as expected. The 4.7 μm and 12.3 μm peaks do not change the wavelength, while the 8.5 μm and 9 μm peaks combined to form one peak. This response peak starts with 8.5 μm at 6 V, then shifts to 8.8 μm when the bias increases. The spectral width of this peak also becomes wider as the bias voltage is increased. Dark current and window current were measured, and the whole stack is BLIP at 90 K up to –3.5 V and +2.7 V, 77 K up to –6.7 V and +6.3 V, and 60 K up to –9.5 V and +9 V. The peak wavelengths corresponding to the BLIP temperatures of 90 K, 77 K, and 60 K are 4.7 μm, 8.8 μm, and 12.3 μm, respectively.

7. Summary

In summary, four multicolor QWIPs are discussed with asymmetrically coupled and multiple stacked quantum well structures. Detailed detector structures and their multicolor capabilities are demonstrated. These four examples are testing samples at single device level, and they showed great promise of using QWIPs for multicolor detection. Specific device design and optimization can be done to tailor the devices for specific applications.

Acknowledgment: Special thanks go to Professor Sheng S. Li, Dr. Xudong Jiang, and Dr. Jung-Chi Chiang for close collaboration, discussion and technical support.

Reference:

1. L. C. West and S. J. Eglash, Appl. Phys. Lett. **46**, 1156(1985).
2. B. F. Levine, J. Appl. Phys. , **74**, R1 (1993).
3. K. L. Tsai, K. H. Chang, C. P. Lee, K. F. Huang, J. S. Tsang, and H. R. Chen, Appl. Phys. Lett. **62**, 3504(1993).
4. M. Z. Tidrow, K. K. Choi, C. Y. Lee, W. H. Chang, F. J. Towner, and J. S. Ahearn, Appl. Phys. Lett., **64**, 1268 (1994).
5. M. Z. Tidrow, J. C. Chiang, Sheng S. Li, and K. Bacher, Appl. Phys. Lett., **70**, 859 (1997).
6. Levine, C. G. Bethea, B. O. Shen , and R. J. Malik, Appl. Phys. Lett. **57**, 383 (1990).
7. R. Parihar, S. A. Lyon, M. Santos, and M. Shayegan, Appl. Phys. Lett. **55**, 2417 (1989).
8. M. Z. Tidrow, K. K. Choi, C. Y. Lee, W. H. Chang, F. J. Towner, and J. S. Ahearn. Appl. Phys. Lett., **64**, 1268 (1994).

9. Jung-Chi Chiang, Sheng S. Li, M. Z. Tidrow, P. Ho, C. M. Tsai, and C. P. Lee, Appl. Phys. Lett. **69**, 2412 (1996).
10. M. Z. Tidrow and K. Bacher, Appl. Phys. Lett, **69**, 3396 (1996).
11. K. Kheng, M. Ramsteiner, J. D. Dalston, F. Fuchs, and P. Koidl, Appl. Phys. Lett. **61**, 666 (1992).
12. H. Wang, Sheng S. Li, and Pin Ho, Appl. Phys. Lett. **62**, 93 (1993).
13. M. Z. Tidrow, K. K. Choi, C. W. Farley, and F. Chang, Appl. Phys. Lett., **65**, 2997 (1994).
14. M. Z. Tidrow, X. D. Jiang, S. S. Li, and K. Bacher, submitted to Appl. Phys. Lett. (1998).